Kato, M[1]., H. Saitsu[1], Y. Murakami[1], K. Kikuchi, S. Watanabe, M. Iai, K. Miya, R. Matsuura, R. Takayama, C. Ohba, M. Nakashima, Y. Tsurusaki, N. Miyake, S. Hamano, H. Osaka, K. Hayasaka, T. Kinoshita and N. Matsumoto.	*PIGA* mutations cause early-onset epileptic encephalopathies and distinctive features.	*Neurology,*	82	1587-1596	2014
Murakami, Y., H. Tawamie, Y. Maeda, C, Buttner, R. Buchert, F. Radwan, S. Schaffer, H. Sticht, M. Aigner, A. Reis, T. Kinoshita and R. A. Jamra.	Null mutation in *PGAP1* impairs GPI-anchor maturation and causes severe non-syndromic recessive intellectual disability.	*PLoS Genet.*	10(5)	e1004320.	2014
Nakashima, M., H. Kashii, Y. Murakami, M. Kato, Y. Tsurusaki, N. Miyake, M. Kubota, T. Kinoshita, H. Saitsu, N. Matsumoto.	Novel compound heterozygous *PIGT* mutations caused multiple congenital anomalies-hypotonia-seizures syndrome 3.	*Neurogenet.,*	15	193-200	2014
Ueda, Y., J. Nishimura, Y. Murakami, S, Kajigaya, T. Kinoshita, Y. Kanakura and N. S. Young.	Paroxysmal nocturnal hemoglobinuria with copy number-neutral 6pLOH in GPI (+) but not in GPI (-) granulocytes.	*Eur. J. Haematol.,*	92:	450-453 DOI: 10.1111/ejh.12253	2014.
Stokes, M., Y. Murakami, Y. Maeda, T. Kinoshita and Y. S. Morita.	New insights to the functions of PIGF, a protein involved in the ethanolamine phosphate transfer steps of glycosylphosphatidylinositol biosynthesis.	*Biochem. J.,*	463(2)	249-256	2014
Fujiwara I, Murakami Y, Niihori T, Kanno J, Hakoda A, Sakamoto O, Okamoto N, Funayama R, Nagashima T, Nakayama K, Kinoshita T, Kure S, Matsubara Y, Aoki Y.	Mutations in PIGL in a patient with Mabry syndrome.	*Am J Med Genet A.*		doi: 10.1002/ajmg.a.36987	2015

村上良子　木下タロウ	知的障害とてんかんを主症状とする新しい疾患—先天性 GPI 欠損症	脳と発達誌	第 47 巻 1 号	5-13	2015
Inoue N, Akazawa T.	IL17A (interleukin 17A).	Atlas of Genetics and Cytogenetics in Oncology and Haematology	19	18-27	2014
Akazawa T, Ohashi T, Nakajima H, Nishizawa Y, Kodama K, Sugiura K, Inaba T, Inoue N.	Development of a dendritic cell-targeting lipopeptide as an immunoadjuvant that inhibits tumor growth without inducing local inflammation.	*Int. J. Cancer*	135	2847-2856	2014
Kodama, K., Higashiyama, M., Okami, J., Tokunaga, T., Fujiwara, A., Inoue, N., Akazawa, T. and Seya, T.	A possible abscopal effect of post-irradiation immunotherapy in two patients with metastatic lung tumors.	*In. Canc. Conf. J.*	3	122-127	2014
Nobusuke Kimura, Yukitoshi Takahashi, Hideo Shigematsu, Katsumi Imai, Hiroko Ikeda, Hideyuki Ootani, Rumiko Takayama, Yukiko Mogami, Noriko Kimura, Koichi Baba, Kazumi Matsuda, Takayasu Tottori, Naotaka Usui, Yushi Inoue	Developmental outcome after surgery in focal cortical dysplasia patients with early-onset epilepsy.	Epilepsy Research	108(10)	1845-1852	2014

Hiroyuki Fujita Hiroyuki, Matsukura S, Watanabe T, Komitsu N, Watanabe Y, Takahashi Y, Kambara T, Ikezawa Z, Aihara M	The serum level of HMGB1 (high mobility group box 1 protein) is preferentially high in drug-induced hypersensitivity syndrome/drug reaction with eosinophilia and systemic symptoms.	British Journal of Dermatology	171(6)	1585-1588	2014
Chiba Yuhei, Katsuse Omi, Fujishiro Hiroshige,Kamada Ayuko, Saito Tomoyuki, Ikura Takahiro, Takahashi Yukitoshi, Kunii Misako, Takeno Mitsuhiro Hirayasu, Yoshio	Lymphopenia Helps Early Diagnosis of Systemic Lupus Erythematosus forPatients with Psychosis as an Initial Symptom	Psycho-somatics.		2013 Sep 23. doi:pii: S0033-3182(13)00136-9. 10.1016/j.psym..	in press
Takahiro Furukawa, Naoko Matsui, Koji Fujita, Ai Miyashiro, Yuishin Izumi, Fumitaka Shimizu, Katsuichi Miyamoto, Yukitoshi Takahashi, Takashi Kanda, Susumu Kusunoki, Ryuji Kaj	Increased proinflammatory cytokines in sera of patients with multifocal motor neuropathy.	J Neurol Sci.		2014 Aug 4. pii: S0022-510X(14)00505-X. doi: 10.1016/j.jns.2014.07.059.	in press
Hiroshi Sakuma, NaoyukiTanuma, Ichiro Kuki, Yukitoshi Takahashi, Masashi Shiomi, Masaharu Hayashi	Intrathecal overproduction of pro-inflammatory cytokines and chemokines in febrile infection related refractory status epilepticus.	Journal of Neurology, Neurosurgery,and Psychiatry			in press
Masaki Yoshimura, Zhang Shouwen, Yuki Ueda, Kazumi Matsuda, Katsumi Imai, Yukitoshi Takahashi, Yushi Inoue	An analysis of epileptic negative myoclonus by magnetoencephalography.	Epilepsy Research			in press

Norimichi Higurashi, Yukitoshi Takahashi, Ayako Kashimada, Yuji Sugawara, Hiroshi Sakuma, Yuko Tomono, Takahito Inoue, Megumi Hoshina, Ruri Satomi, Masaharu Ohfu, Kazuya Itomi, Kyoko Takano, Tomoko Kirino, Shinichi Hirose	Immediate suppression of seizure clusters by corticosteroids in PCDH19 female epilepsy.	Seizure			in press
高橋幸利、森達夫、大星大観、東本和紀、	神経疾患と NMDA 型グルタミン酸受容	日本小児科学会誌	118(12)	1695-1707	2014
高橋幸利、木水友一、小池敬義、堀野朝子、	免疫性神経疾患-基礎・臨床研究の最新	日本臨床増刊号			印刷中

Ⅳ．　研究成果の刊行物・別刷

Neurogenetics (2014) 15:85–92
DOI 10.1007/s10048-013-0384-7

ORIGINAL ARTICLE

PIGN mutations cause congenital anomalies, developmental delay, hypotonia, epilepsy, and progressive cerebellar atrophy

Chihiro Ohba · Nobuhiko Okamoto · Yoshiko Murakami · Yasuhiro Suzuki · Yoshinori Tsurusaki · Mitsuko Nakashima · Noriko Miyake · Fumiaki Tanaka · Taroh Kinoshita · Naomichi Matsumoto · Hirotomo Saitsu

Received: 2 November 2013 / Accepted: 10 November 2013 / Published online: 20 November 2013
© Springer-Verlag Berlin Heidelberg 2013

Abstract Defects of the human glycosylphosphatidylinositol (GPI) anchor biosynthetic pathway show a broad range of clinical phenotypes. A homozygous mutation in *PIGN*, a member of genes involved in the GPI anchor-synthesis pathway, was previously reported to cause dysmorphic features, multiple congenital anomalies, severe neurological impairment, and seizure in a consanguineous family. Here, we report two affected siblings with compound heterozygous *PIGN* mutations [c.808T >C (p.Ser270Pro) and c.963G >A] showing congenital anomalies, developmental delay, hypotonia, epilepsy, and progressive cerebellar atrophy. The c.808C >T mutation altered an evolutionarily conserved amino acid residue (Ser270), while reverse transcription-PCR and sequencing demonstrated that c.963G >A led to aberrant splicing, in which two mutant transcripts with premature stop codons (p.Ala322Valfs*24 and p.Glu308Glyfs*2) were generated. Expression of GPI-anchored proteins such as CD16 and CD24 on granulocytes from affected siblings was

Chihiro Ohba, Nobuhiko Okamoto, and Yoshiko Murakami contributed equally

Electronic supplementary material The online version of this article (doi:10.1007/s10048-013-0384-7) contains supplementary material, which is available to authorized users.

C. Ohba · Y. Tsurusaki · M. Nakashima · N. Miyake · N. Matsumoto · H. Saitsu (✉)
Department of Human Genetics, Graduate School of Medicine, Yokohama City University, 3-9 Fukuura, Kanazawa-ku, Yokohama 236-0004, Japan
e-mail: hsaitsu@yokohama-cu.ac.jp

C. Ohba
e-mail: t116017g@yokohama-cu.ac.jp

Y. Tsurusaki
e-mail: tsurusak@yokohama-cu.ac.jp

M. Nakashima
e-mail: mnakashi@yokohama-cu.ac.jp

N. Miyake
e-mail: nmiyake@yokohama-cu.ac.jp

N. Matsumoto
e-mail: naomat@yokohama-cu.ac.jp

C. Ohba · F. Tanaka
Department of Clinical Neurology and Stroke Medicine, Yokohama City University, Yokohama 236-0004, Japan

F. Tanaka
e-mail: ftanaka@yokohama-cu.ac.jp

N. Okamoto
Department of Medical Genetics, Osaka Medical Center and Research Institute for Maternal and Child Health, Izumi 594-1101, Japan
e-mail: okamoto@osaka.email.ne.jp

Y. Murakami · T. Kinoshita
Department of Immunoregulation, Research Institute for Microbial Diseases, Osaka University, Osaka 565-0871, Japan

Y. Murakami
e-mail: yoshiko@biken.osaka-u.ac.jp

T. Kinoshita
e-mail: tkinoshi@biken.osaka-u.ac.jp

Y. Murakami · T. Kinoshita
World Premier International Immunology Frontier Research Center, Osaka University, Osaka 565-0871, Japan

Y. Suzuki
Department of Pediatric Neurology, Osaka Medical Center and Research Institute for Maternal and Child Health, Osaka, Japan
e-mail: yasuzuki@mch.pref.osaka.jp

significantly decreased, and expression of the GPI-anchored protein CD59 in *PIGN*-knockout human embryonic kidney 293 cells was partially or hardly restored by transient expression of p.Ser270Pro and p.Glu308Glyfs*2 mutants, respectively, suggesting severe and complete loss of PIGN activity. Our findings confirm that developmental delay, hypotonia, and epilepsy combined with congenital anomalies are common phenotypes of *PIGN* mutations and add progressive cerebellar atrophy to this clinical spectrum.

Keywords Cerebellar atrophy · Compound heterozygous mutation · Glycosylphosphatidylinositol anchor · *PIGN*

Introduction

Defects of the biosynthetic pathway of the glycosylphosphatidylinositol (GPI) anchor cause broad clinical phenotypes [1]. The products of more than 20 genes in the phosphatidylinositol glycan (PIG) family are involved in GPI biosynthesis, whereas post-GPI-attachment to proteins (PGAP) gene products play a role in the structural remodeling of GPI glycan and lipid portions [2]. Mutations in eight genes involved in GPI biosynthesis and remodeling (*PIGA*, *PIGM*, *PIGN*, *PIGV*, *PIGL*, *PIGO*, *PIGT*, and *PGAP2*) have been identified in individuals with neurological abnormalities [1, 3–5], of which *PIGN* controls the addition of phosphoethanolamine to the first mannose in GPI [6]. To date, only one homozygous *PIGN* mutation has been reported to cause dysmorphic features, multiple congenital anomalies, severe neurological impairment, and seizures in a consanguineous family [7]. Here, we report a family with two affected siblings, possessing compound heterozygous *PIGN* mutations. Detailed clinical information and molecular and functional analyses are presented.

Patients and methods

Patients

We analyzed two affected siblings and their parents. Experimental protocols were approved by the Institutional Review Board of Yokohama City University School of Medicine. Clinical information and peripheral blood samples were acquired from the family members after obtaining written informed consent. Patient clinical features are summarized in Table 1. They showed dysmorphic facial features, developmental delay, intellectual disability, hypotonia, vertical nystagmus, and epilepsy.

Patient 1

This 9-year-old girl was born to nonconsanguineous healthy parents as a second child after 39 weeks of gestation (Fig. 1a). Her birth weight was 3,390 g [+1.40 standard deviation (SD)], body length of 49 cm (−0.03 SD), and head circumference of 35 cm (+1.35 SD). At 1 month of age, she showed vertical nystagmus without eye pursuit. She was hypotonic, and severe developmental delay was evident from early infancy. She was unable to control her head or utter words at 9 years of age. Abdominal echogram revealed bilateral vesicoureteral reflux as a cause of repeated urinary tract infections. Complex partial seizures developed at 8 months of age and were controlled by antiepileptic drugs. Tube feeding by gastrostomy was necessary for poor appetite at the age of 2 years.

Several dysmorphic features (prominent occiput, bitemporal narrowing, epicanthal folds, open mouth, tented upper lip, high arched palate, micrognathia, and deep plantar groove) were noted (Fig. 1b), but hypoplasia was absent from fingers and fingernails. Initial brain magnetic resonance imaging (MRI) at 6 months of age was normal, but cerebellar atrophy was observed at 2 and 6 years of age (Fig. 1c–f).

At present, her height is 122 cm (+1.1 SD), weight of 18.4 kg (−1.2 SD), and head circumference of 51.4 cm (−0.3 SD). Generalized muscle weakness and nystagmus were neurologically recognized. Laboratory examination showed a normal profile, including blood cell count and blood smear, renal and liver function, total bilirubin, uric acid, albumin, serum electrolytes, lactate, pyruvate, ammonia, amino acids, blood gasses, thyroid function, and cerebrospinal fluid study. Her serum alkaline phosphatase (ALP) activity has been normal for her age since infancy. Metabolic disorder screening including organic acid analysis, lysosomal enzymes, and mass spectrometry of transferrin was normal. G-banded analysis showed a normal karyotype (46, XX).

Patient 2

This 2-year-old boy was born after 37 weeks of gestation as a younger brother to patient 1 (Fig. 1a). His birth weight was 3,252 g (+1.3 SD), body length of 50 cm (+1.2 SD), and head circumference of 35 cm (+1.6 SD). He also showed vertical nystagmus at 1 month of age. Complex partial seizures developed at 5 months of age. He was hypotonic, and his developmental milestones were severely delayed with no head control at 1 year and 10 months of age. At present, his height is 92.3 cm (+2.5 SD), weight of 10.9 kg (−0.6 SD), and head circumference of 48.8 cm (+0.4 SD). He showed similar dysmorphic features to patient 1. Brain MRI at 2 months of age revealed no significant abnormalities.

Table 1 Clinical features of patients with *PIGN* mutations

Patient	1	2	Reported by Maydan et al. [7]							
			V-1	V-2	V-4	V-5	V-8	V-9	V-10	Total
Age (years)	9	2	N.D.	Diseased at 14	Diseased at 1	Diseased at 5	Diseased at 3	Diseased at 17	Diseased at 39	
Sex	Female	Male	Male	Male	Male	Female	Female	Female	Male	
Size at birth (percentile)										
Weight (g)	3,390 (90–97)	3,252 (90–97)	3,566 (95)	4,065 (97)	3,850 (95)	3,410 (40)	4,250 (99)	4,300 (98)	4,800 (>99)	
Head circumference (cm)	35 (90)	35 (90–97)	37 (>97)	37 (97)	35.5 (75)	34.5 (10)	N.D.	N.D.	N.D.	
Abnormalities										
Facial features	+	+	+	+	+	+	+	+	+	9/9
Fingers/foot	+	+	+	+	+	-	–	+	+	6/9
Heart	–	–	+	+	+	+	–	+	–	5/9
Urinary tract	+	–	+	+	+	–	–	–	–	4/9
Gastrointestinal tract	GER	–	GER	GER	Anal stenosis	Imperforate anus, ano-vestibular fistula, GER	–	Feeding and swallowing difficulties	Feeding and swallowing difficulties	7/9
Neurological features										
Developmental delay	+	+	+	+	+	+	+	+	+	9/9
Hypotonia	+	+	+	+	+	+	+	+	+	9/9
Nystagmus	+	+	+	+	–	+	–	+	+	7/9
Tremor	+	+	+	+	+	+	+	–	–	7/9
Seizure	+	+	+	–	+	+	+	+	+	8/9
Brain CT	Normal	Normal	Normal	N.D.	Normal	Multiple small subdural hematomas	N.D.	N.D.	N.D.	1/5
Brain MRI				N.D.	N.D.		N.D.	N.D.	N.D.	
Delayed myelination	+	–	–			+				2/4
Thin corpus callosum	–	–	–			+				1/4
Cerebellar atrophy	+	–	Minimal loss of vermis parenchyma			–				1/4
Enlargement of the ventricle	+	–	–			+ (Mild)				2/4

GER Gastroesophageal reflux, *N.D.* not determined

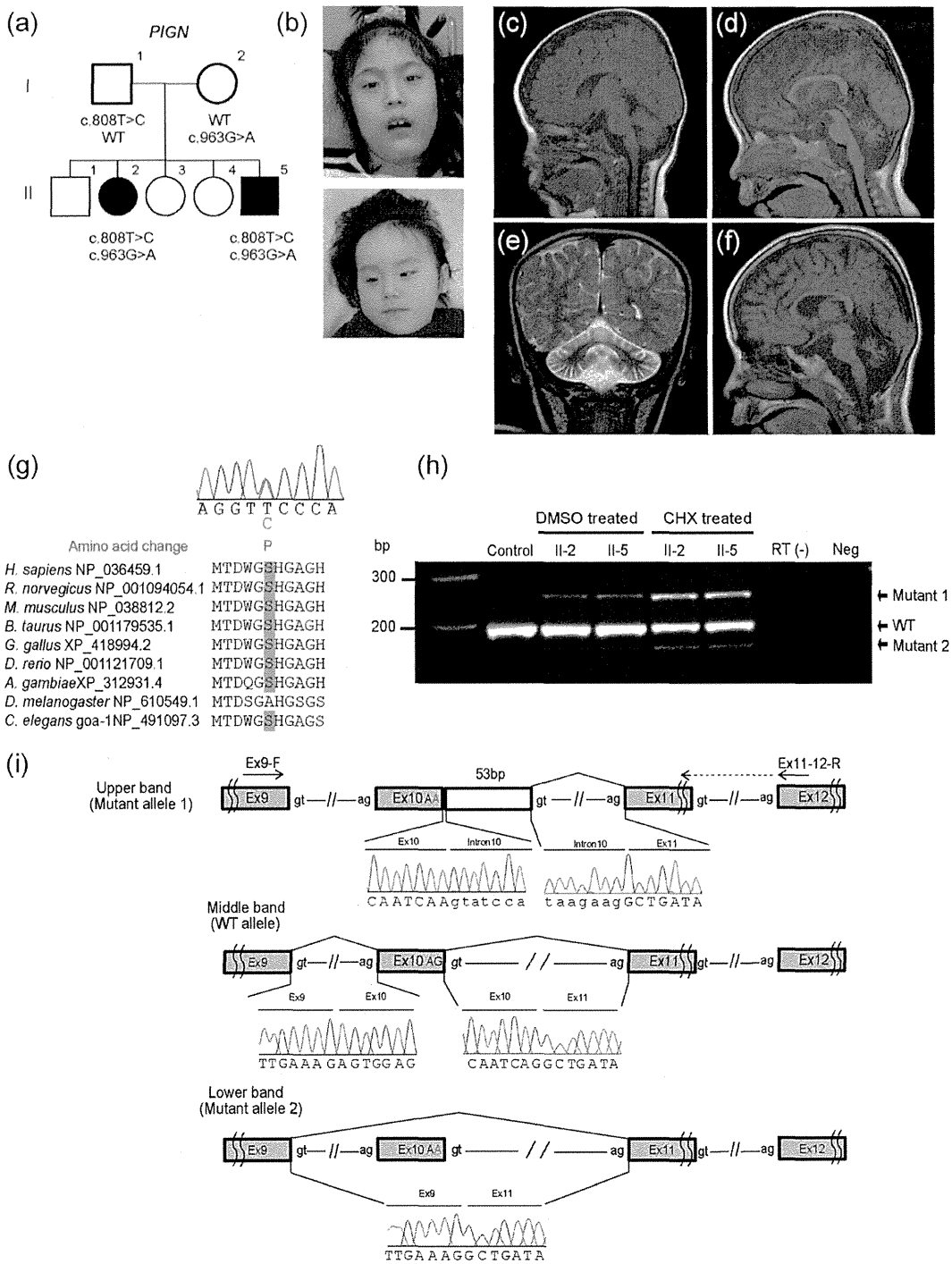

Whole exome sequencing (WES)

Genomic DNA was isolated from peripheral blood leukocytes, captured using the SureSelect Human All Exon v4 Kit (51 Mb; Agilent Technologies, Santa Clara, CA), and sequenced on an Illumina HiSeq2000 (Illumina, San Diego, CA) with 101 bp paired-end reads. Data processing, variant calling, and variant annotation were performed as previously described [8].

◀ **Fig. 1** **a** Familial pedigree and mutations. **b** Photographs of the faces of patient 1 (*upper*) and patient 2 (*lower*). Frontal narrow temporal, frontal bossing, hypertelorism, epicanthal folds, down-slanting palpebral fissures, high nasal bridge, bilateral low set ears, thin philtrum, downturned mouth, and microretrognathia are noted in both patients. **c**, **d**, **f** T1-weighted midline sagittal images and **e** T2-weighted coronal images of patient 1 (**c** at 6 months, **d** and **e** at 2 years, and **i** at 6 years). Progressive vermis atrophy (**c**, **d**, **f**) and hemispheres atrophy (**e**) were observed. **g** Sequence chromatography showing heterozyogous c.808C >T mutation, which alters an evolutionarily conserved amino acid. Homologous sequences were aligned using CLUSTALW. **h** RT-PCR analysis using cDNA of LCLs derived from two patients (II-2 and II-5) and a control. **i** Schematic representation of wild-type (WT) and mutant transcripts and primers used for the analysis. Primer of ex11-12-R spans exons 11 and 12. A single band (200 bp), corresponding to the WT allele, was amplified using control cDNA. Upper and lower bands were detected from patient cDNA. The upper band (253 bp) has a 53-bp insertion of intron 10 sequences, leading to a frameshift mutation. The lower band has a 41-bp deletion of the entire exon 10, also leading to a frameshift mutation

Reverse transcriptase-PCR

Lymphoblastoid cell lines (LCLs) were established from the two patients. RT-PCR using total RNA extracted from LCLs was performed as previously described [9].

Briefly, total RNA was extracted using the RNeasy Plus Mini kit (Qiagen, Tokyo, Japan) from LCLs with or without incubation in 30 μM cycloheximide (CHX; Sigma, Tokyo, Japan) for 4 h. Four micrograms of total RNA was subjected to reverse transcription, and 2 μl cDNA was used for PCR. Primer sequences were ex9-F (5′-TCCTTTAGTCACTTGG GGAGCTGGA-3′) and ex11-12-R (5′-AATCCACAGGAA GGATTCCCACTGA-3′) (Supplementary Table 1). PCR products were electrophoresed on a 10 % polyacrylamide gel and sequenced. PCR bands were purified by the E.Z.N.A. poly-Gel DNA Extraction kit (Omega Bio-Tek, Norcross, GA).

Fluorescence-activated cell sorting (FACS) analysis

Surface expression of GPI-anchored proteins (GPI-APs) was determined by staining cells with Alexa 488-conjugated inactivated aerolysin [fluorescently-labeled inactive toxin aerolysin (FLAER); Protox Biotech, Victoria, BC, Canada] and appropriate primary antibodies: mouse anti-decay accelerating factor (DAF; IA10), −CD16 (3G8), −CD24 (ML5), −CD59 (5H8), and −CD48 (BJ40) followed by a PE-conjugated anti-mouse IgG antibody (3G8, ML5, BJ40, and secondary antibodies; BD Biosciences, Franklin Lakes, NJ). Cells were analyzed by flow cytometry (Cant II; BD Biosciences) with Flowjo software (v9.5.3, Tommy Digital, Tokyo, Japan).

Functional analysis in HEK293 cells

PIGN-knockout cells were generated from HEK293 cells using the CRISPR/Cas System [10]. We obtained the human codon-optimized *Streptococcus pyogenes* Cas9 and chimeric guide RNA expression plasmid pX330 from Addgene (Cambridge, MA). The seed sequence for the SpCas9 target site in *PIGN* exon 4 (CCA-GGTCATGTAGCTCTGATAGC) was selected and a pair of annealed oligos designed according to this sequence and cloned into the *Bbs* I sites of pX330. HEK293 cells were transfected with pX330 containing the target site using Lipofectamine 2000 (Invitrogen, Carlsbad, CA). Cells were stained with anti-CD59 antibody 14 days after transfection, and *PIGN*-knockout clones were obtained by limiting dilution.

PIGN-knockout HEK293 cells (clone PIGNKO2-12) were transiently transfected with a wild-type or mutant (S290P or exon 10 skipping) *PIGN* cDNA cloned into the SRα promoter-driven expression vector pME HA-PIGN. Restoration of the surface expression of CD59, DAF, and GPI-APs was assessed 2 days later by flow cytometry.

Results

WES detected 288 and 292 rare protein-altering and splice-site variants in patients 1 and 2, respectively. We filtered out common single nucleotide polymorphisms (SNPs) that met the following two criteria: variants showing minor allele frequencies ≥1 % in dbSNP 135 and variants found in more than two of our in-house 406 control exomes (Supplementary Table 2). All genes were surveyed for compound heterozygous or homozygous mutations consistent with an autosomal recessive trait, and only *PIGN* (GenBank accession number NM_176787.4) met this criterion, possessing compound heterozygous mutations in two patients. The missense mutation c.808T >C (p.Ser270Pro) was inherited from the patients' father, while c.963G >A is a synonymous mutation inherited from their mother but located at the last base of exon 10 (Fig. 1i). Neither of the two mutations was present in the 6,500 exomes sequenced by the National Heart, Lung, and Blood Institute exome project. In our 406 in-house control exomes, c.808T >C was absent, but c.963G >A was found in one, as a heterozygous mutation. c.808T >C occurred at evolutionary conserved amino acids (Fig. 1g) and was predicted to be pathogenic using online software (Supplementary Table 3). To examine the actual effects of c.963G >A on splicing, RT-PCR was performed (Fig. 1h, i) and a single band (200 bp) corresponding to the wild-type *PIGN* allele was amplified from control LCL cDNA template (Fig. 1h). By contrast, two aberrant faint bands were detected in addition to a wild-type band from patient cDNA (Fig. 1h). Sequencing of the upper aberrant band indicated a 53-bp insertion of intron 10 sequences that had

used a cryptic splice donor site within intron 10, producing a premature stop codon (p.Ala322Valfs*24). Sequencing of the lower band demonstrated the deletion of exon 10 from wild-type *PIGN* mRNA, also producing a premature stop codon (p.Glu308Glyfs*2). Therefore, these two mutant transcripts are likely to be degraded by nonsense-mediated mRNA decay (NMD). In fact, CHX treatment, which inhibits NMD, increased the intensity of the aberrant bands, suggesting that NMD was indeed involved.

To examine the functional impairment of *PIGN* caused by compound heterozygous mutations, the surface expression of various GPI-APs was analyzed by flow cytometry. CD16 and CD24 expression on blood granulocytes was decreased to 26–54 % of normal levels in both patients (Fig. 2a). No abnormal GPI-APs expression was observed on LCLs from either patient (Supplementary Fig. 1).

Transient expression of p.Ser270Pro and exon 10 skipping (p.Glu308Glyfs*2) mutants in *PIGN*-knockout HEK293 cells, in which expression of GPI-APs CD59 was decreased, was confirmed by immunoblotting. Expression of the exon 10 skipping mutant was decreased compared with that of wild-type and p.Ser270Pro mutant (Supplementary Fig. 2). CD59 expression was only partially or hardly restored by the transient expression of p.Ser270Pro and exon 10 skipping mutants, respectively, suggesting severe or complete loss of PIGN activity (Fig. 2b).

Discussion

Herein, we report a second family with *PIGN* mutations that showed clinical features common to a previous affected family, including congenital anomalies, developmental delay, hypotonia, and epilepsy [7]. In addition, nystagmus was an early symptom of patients in this study and was also observed in five of seven patients previously [7]. Of note, progressive cerebellar atrophy was observed in the current patient 1, and this appears to be a novel phenotype associated with *PIGN*

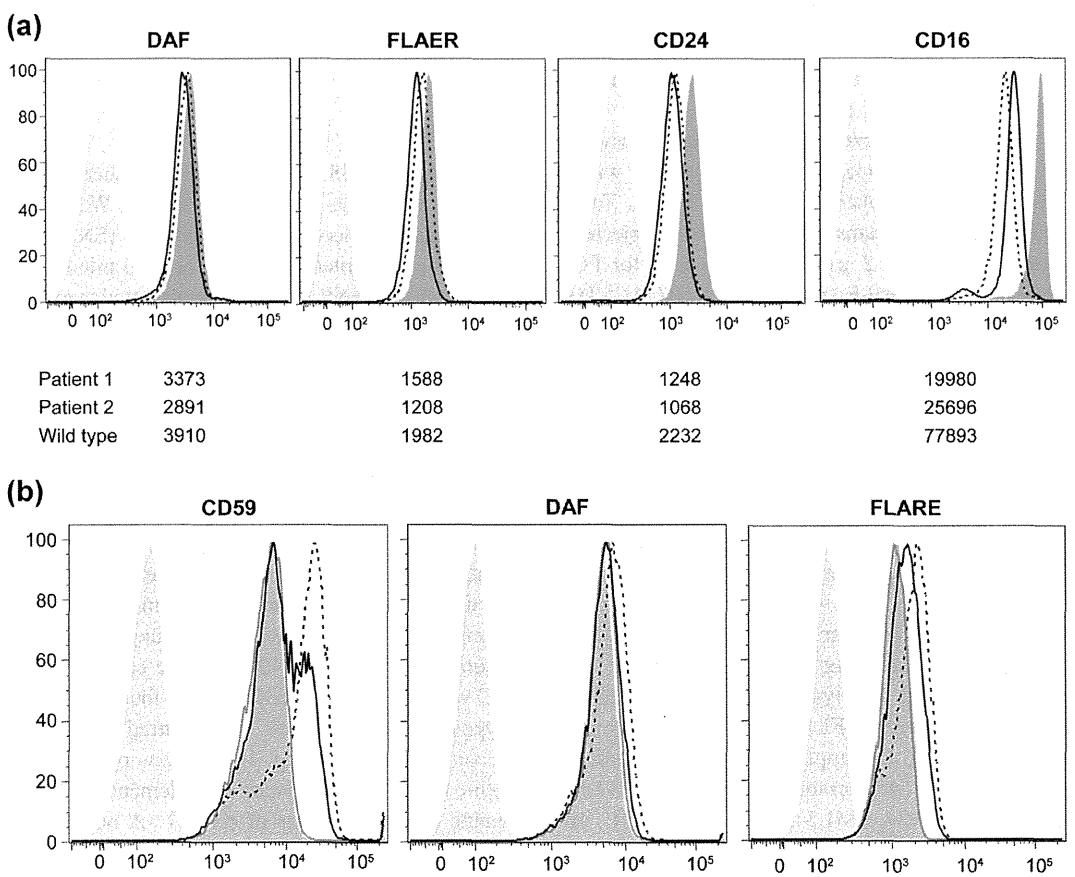

Fig. 2 **a** Surface expression of various GPI-APs on patient granulocytes (patient 1: *dotted lines*, patient 2: *solid lines*), a normal control (*dark shadow*) and an isotype control (*light shadows*). Numbers represent mean fluorescent intensities. Expression of DAF and FLAER in both patients did not significantly change compared with the control. However, CD16 and CD24 expression decreased to 26–54 % of normal levels. **b** *PIGN*-knockout HEK293 cells were transiently transfected with wild type (*dotted lines*) or mutants (exon 10 skipping: *gray line*, p.Ser270Pro: *black line*) of pME HA-PIGN vectors. Empty vector: *dark shadow*, isotype control: *light shadow*. Expression of CD59 was only partially or hardly restored by p.Ser270Pro and exon 10-skipping vectors, respectively

mutations as two patients examined by MRI showed no cerebellar atrophy but only minimal loss of vermis parenchyma in one patient (patient V-1) in the previous report [7].

PIGN is involved in the addition of phosphoethanolamine to the first mannose in GPI [6]. In *Pign*-knockout mouse F9 embryonal carcinoma cells, the first mannose in GPI precursors is not modified by phosphoethanolamine. Nevertheless, further biosynthetic steps continue and the cell surface expression of GPI-anchored proteins is only partially affected [6], suggesting that this modification may not be essential for GPI-anchored protein biosynthesis [6]. By contrast, the *gonzo* mouse line, which harbors the splice donor site mutation in *Pign*, showed abnormal forebrain development resembling holoprosencephaly [11], and patients with *PIGN* mutations show severe phenotypes such as multiple congenital anomalies, neurological impairment, and even lethality [7]; this indicates that particular defects of *PIGN*/*Pign* cause abnormal development both in mice and humans. Although the overall amount of GPI-anchored proteins might not be significantly affected by *PIGN* defects, as revealed by the minimal decrease in DAF and FLAER expression on patient granulocytes in the present study, changes to a subset of GPI-anchored proteins such as CD16 and CD24 can be sufficient to cause severe neurological phenotypes. Additionally or alternatively, GPI-APs expressed on PIGN-defective cells lack the phosphoethanolamine-side branch, and this abnormal structure of the glycan part of the anchor might affect functions of GPI-APs. Functional analysis using neuronal cells may provide novel insights into the pathogenesis of neurological phenotypes caused by *PIGN* mutations.

Seven genes (*PIGA*, *PIGM*, *PIGN*, *PIGV*, *PIGL*, *PIGO*, and *PGAP2*) have been identified as being mutated in patients with neurological abnormalities. Mutations in three of these (*PIGV*, *PIGO*, and *PGAP2*) cause hyperphosphatasia [3, 12–14], suggesting that ALP is a useful marker for suspected GPI anchor-synthesis pathway deficiencies. However, mutations of the other four genes (*PIGA*, *PIGM*, *PIGN*, and *PIGL*) did not cause hyperphosphatasia [7, 14, 15], so clinical diagnosis might be difficult in the absence of specific biomarkers. Even in clinically unsuspected patients, WES may identify mutations in genes involved in the GPI anchor-synthesis pathway. Current advances in next generation sequencing should find more comprehensive answers for unsolved GPI anchor-related diseases.

Acknowledgments We would like to thank patients and their parents for their participation in this study. We also thank Nobuko Watanabe and Kana Miyanagi for technical assistance. This work was supported by the Ministry of Health, Labour, and Welfare of Japan; a Grant-in-Aid for Scientific Research (A), (B), and (C) from the Japan Society for the Promotion of Science (A: 24249019, B: 25293085 25293235, C: 23590363); the Takeda Science Foundation; the Japan Science and Technology Agency; the Strategic Research Program for Brain Sciences (11105137); and a Grant-in-Aid for Scientific Research on Innovative Areas (Transcription Cycle, Exploring molecular basis for brain diseases based on personal genomics) from the Ministry of Education, Culture, Sports, Science, and Technology of Japan (12024421, 25129705).

References

1. Freeze HH, Eklund EA, Ng BG, Patterson MC (2012) Neurology of inherited glycosylation disorders. Lancet Neurol 11(5):453–466. doi:10.1016/s1474-4422(12)70040-6
2. Maeda Y, Kinoshita T (2011) Structural remodeling, trafficking and functions of glycosylphosphatidylinositol-anchored proteins. Prog Lipid Res 50(4):411–424. doi:10.1016/j.plipres.2011.05.002
3. Hansen L, Tawamie H, Murakami Y, Mang Y, ur Rehman S, Buchert R, Schaffer S, Muhammad S, Bak M, Nothen MM, Bennett EP, Maeda Y, Aigner M, Reis A, Kinoshita T, Tommerup N, Baig SM, Abou Jamra R (2013) Hypomorphic mutations in *PGAP2*, encoding a GPI-anchor-remodeling protein, cause autosomal-recessive intellectual disability. Am J Hum Genet 92(4):575–583. doi:10.1016/j.ajhg.2013.03.008
4. Krawitz PM, Murakami Y, Riess A, Hietala M, Kruger U, Zhu N, Kinoshita T, Mundlos S, Hecht J, Robinson PN, Horn D (2013) *PGAP2* mutations, affecting the GPI-anchor-synthesis pathway, cause hyperphosphatasia with mental retardation syndrome. Am J Hum Genet 92(4):584–589. doi:10.1016/j.ajhg.2013.03.011
5. Kvarnung M, Nilsson D, Lindstrand A, Korenke GC, Chiang SC, Blennow E, Bergmann M, Stodberg T, Makitie O, Anderlid BM, Bryceson YT, Nordenskjold M, Nordgren A (2013) A novel intellectual disability syndrome caused by GPI anchor deficiency due to homozygous mutations in *PIGT*. J Med Genet 50(8):521–528. doi:10.1136/jmedgenet-2013-101654
6. Hong Y, Maeda Y, Watanabe R, Ohishi K, Mishkind M, Riezman H, Kinoshita T (1999) Pig-n, a mammalian homologue of yeast Mcd4p, is involved in transferring phosphoethanolamine to the first mannose of the glycosylphosphatidylinositol. J Biol Chem 274(49):35099–35106
7. Maydan G, Noyman I, Har-Zahav A, Neriah ZB, Pasmanik-Chor M, Yeheskel A, Albin-Kaplanski A, Maya I, Magal N, Birk E, Simon AJ, Halevy A, Rechavi G, Shohat M, Straussberg R, Basel-Vanagaite L (2011) Multiple congenital anomalies-hypotonia-seizures syndrome is caused by a mutation in *PIGN*. J Med Genet 48(6):383–389. doi:10.1136/jmg.2010.087114
8. Saitsu H, Nishimura T, Muramatsu K, Kodera H, Kumada S, Sugai K, Kasai-Yoshida E, Sawaura N, Nishida H, Hoshino A, Ryujin F, Yoshioka S, Nishiyama K, Kondo Y, Tsurusaki Y, Nakashima M, Miyake N, Arakawa H, Kato M, Mizushima N, Matsumoto N (2013) *De novo* mutations in the autophagy gene *WDR45* cause static encephalopathy of childhood with neurodegeneration in adulthood. Nat Genet. doi:10.1038/ng.2562
9. Saitsu H, Kato M, Okada I, Orii KE, Higuchi T, Hoshino H, Kubota M, Arai H, Tagawa T, Kimura S, Sudo A, Miyama S, Takami Y, Watanabe T, Nishimura A, Nishiyama K, Miyake N, Wada T, Osaka H, Kondo N, Hayasaka K, Matsumoto N (2010) *STXBP1* mutations in early infantile epileptic encephalopathy with suppression-burst pattern. Epilepsia 51(12):2397–2405. doi:10.1111/j.1528-1167.2010.02728.x
10. Cong L, Ran FA, Cox D, Lin S, Barretto R, Habib N, Hsu PD, Wu X, Jiang W, Marraffini LA, Zhang F (2013) Multiplex genome engineering using CRISPR/Cas systems. Science 339(6121):819–823. doi:10.1126/science.1231143
11. McKean DM, Niswander L (2012) Defects in GPI biosynthesis perturb Cripto signaling during forebrain development in two new mouse models of holoprosencephaly. Biology open 1(9):874–883. doi:10.1242/bio.20121982
12. Freeze HH (2013) Understanding human glycosylation disorders: biochemistry leads the charge. J Biol Chem 288(10):6936–6945. doi:10.1074/jbc.R112.429274

13. Krawitz PM, Murakami Y, Hecht J, Kruger U, Holder SE, Mortier GR, Delle Chiaie B, De Baere E, Thompson MD, Roscioli T, Kielbasa S, Kinoshita T, Mundlos S, Robinson PN, Horn D (2012) Mutations in *PIGO*, a member of the GPI-anchor-synthesis pathway, cause hyperphosphatasia with mental retardation. Am J Hum Genet 91(1):146–151. doi:10.1016/j.ajhg.2012.05.004
14. Almeida AM, Murakami Y, Layton DM, Hillmen P, Sellick GS, Maeda Y, Richards S, Patterson S, Kotsianidis I, Mollica L, Crawford DH, Baker A, Ferguson M, Roberts I, Houlston R, Kinoshita T, Karadimitris A (2006) Hypomorphic promoter mutation in *PIGM* causes inherited glycosylphosphatidylinositol deficiency. Nat Med 12(7):846–851. doi:10.1038/nm1410
15. Johnston JJ, Gropman AL, Sapp JC, Teer JK, Martin JM, Liu CF, Yuan X, Ye Z, Cheng L, Brodsky RA, Biesecker LG (2012) The phenotype of a germline mutation in *PIGA*: the gene somatically mutated in paroxysmal nocturnal hemoglobinuria. Am J Hum Genet 90(2):295–300. doi:10.1016/j.ajhg.2011.11.031

Human Molecular Genetics, 2014, Vol. 23, No. 12 **3200–3211**
doi:10.1093/hmg/ddu030
Advance Access published on January 25, 2014

Clinical whole-genome sequencing in severe early-onset epilepsy reveals new genes and improves molecular diagnosis

Hilary C. Martin[1,†], Grace E. Kim[2,†], Alistair T. Pagnamenta[1,3], Yoshiko Murakami[4], Gemma L. Carvill[5], Esther Meyer[6,7], Richard R. Copley[1,3], Andrew Rimmer[1], Giulia Barcia[8], Matthew R. Fleming[2], Jack Kronengold[2], Maile R. Brown[2], Karl A. Hudspith[1,3], John Broxholme[1], Alexander Kanapin[1], Jean-Baptiste Cazier[1], Taroh Kinoshita[4], Rima Nabbout[8], The WGS500 Consortium[‡], David Bentley[9], Gil McVean[1], Sinéad Heavin[10], Zenobia Zaiwalla[11], Tony McShane[12], Heather C. Mefford[5], Deborah Shears[13], Helen Stewart[13], Manju A. Kurian[6], Ingrid E. Scheffer[10], Edward Blair[13], Peter Donnelly[1,¶], Leonard K. Kaczmarek[2,¶] and Jenny C. Taylor[1,3,¶,*]

[1]Wellcome Trust Centre for Human Genetics, University of Oxford, Oxford, UK, [2]Departments of Cellular and Molecular Physiology and Pharmacology, Yale University School of Medicine, New Haven, CT, USA, [3]NIHR Biomedical Research Centre, Oxford, UK, [4]Department of Immunoregulation, Research Institute for Microbial Diseases, Osaka University, Osaka, Japan, [5]Department of Pediatrics, Division of Genetic Medicine, University of Washington, Seattle, WA, USA, [6]Neurosciences Unit, UCL-Institute of Child Health, London, UK, [7]Department of Neurology, Great Ormond Street Hospital, London, UK, [8]Department of Paediatric Neurology, Centre de Reference Epilepsies Rares, Hôpital Necker-Enfants Malades, Paris, France, [9]Illumina Inc., San Diego, CA, USA, [10]Departments of Medicine and Paediatrics, Florey Institute, The University of Melbourne, Austin Health and Royal Children's Hospital, Melbourne, VIC, Australia, [11]Department of Clinical Neurophysiology, John Radcliffe Hospital, Oxford, UK, [12]Department of Paediatrics, Children's Hospital Oxford, John Radcliffe Hospital, Oxford, UK and [13]Department of Clinical Genetics, Oxford University Hospitals NHS Trust, Oxford, UK

Received September 20, 2013; Revised and Accepted January 20, 2014

In severe early-onset epilepsy, precise clinical and molecular genetic diagnosis is complex, as many metabolic and electro-physiological processes have been implicated in disease causation. The clinical phenotypes share many features such as complex seizure types and developmental delay. Molecular diagnosis has historically been confined to sequential testing of candidate genes known to be associated with specific sub-phenotypes, but the diagnostic yield of this approach can be low. We conducted whole-genome sequencing (WGS) on six patients with severe early-onset epilepsy who had previously been refractory to molecular diagnosis, and their parents. Four of these patients had a clinical diagnosis of Ohtahara Syndrome (OS) and two patients had severe non-syndromic early-onset epilepsy (NSEOE). In two OS cases, we found *de novo* non-synonymous mutations in the genes *KCNQ2* and *SCN2A*. In a third OS case, WGS revealed paternal isodisomy for chromosome 9, leading to identification of the causal homozygous missense variant in *KCNT1*, which produced a substantial increase in potassium channel current. The fourth OS patient had a recessive mutation in *PIGQ* that led to exon skipping and defective glycophosphatidyl inositol biosynthesis. The two patients with NSEOE had likely pathogenic *de novo* mutations in *CBL* and *CSNK1G1*, respectively. Mutations in these

*To whom correspondence should be addressed at: Genomic Medicine Theme, Oxford Biomedical Research Centre, Wellcome Trust Centre for Human Genetics, Oxford OX3 7BN, UK. Tel: +44 1865287633; Fax: +44 1865287770; Email: jenny@well.ox.ac.uk
†These authors contributed equally to this work.
‡A full list of members is provided in the Supplementary Material.
¶These authors jointly directed this work.

© *The Author 2014. Published by Oxford University Press.*
This is an Open Access article distributed under the terms of the Creative Commons Attribution License (http://creativecommons.org/licenses/by/3.0/), which permits unrestricted reuse, distribution, and reproduction in any medium, provided the original work is properly cited.

Downloaded from http://hmg.oxfordjournals.org/ at Osaka Daigaku Ningen on March 17, 2015

genes were not found among 500 additional individuals with epilepsy. This work reveals two novel genes for OS, *KCNT1* and *PIGQ*. It also uncovers unexpected genetic mechanisms and emphasizes the power of WGS as a clinical tool for making molecular diagnoses, particularly for highly heterogeneous disorders.

INTRODUCTION

Many recent studies have successfully used whole-exome or whole-genome sequencing (WES, WGS) to uncover the genetic basis of rare disorders (reviewed by 1,2), primarily in a research context. In addition, WES and WGS offer potentially revolutionary approaches to molecular diagnosis for patients in a clinical setting. In order to assess the possible clinical utility of WGS, we have sequenced the genomes of 500 individuals with a variety of medical conditions, including cancer, immunological disease and rare, putatively monogenic syndromes (3–5). As part of this 'WGS500 project', we sequenced six patients with severe early-onset epilepsy who had been previously refractory to molecular diagnosis.

Severe early-onset epilepsy is a good candidate for WGS as it is a challenging disorder to understand mechanistically. It represents a broad spectrum of phenotypes which are highly heterogeneous at the clinical and molecular levels (6). While some causative genes have been identified for many of these subphenotypes, the limitations of current technologies mean that genetic testing is largely confined to the genes associated with the specific presenting phenotype. However, it is increasingly being recognized that a given gene can cause multiple phenotypes (6), and that more comprehensive genetic testing may improve molecular diagnostic yield (7). This is useful clinically not only because it can help make or confirm a diagnosis, but also because it may allow counseling on recurrence risk and prenatal testing.

In its most severe form, early-onset epilepsy involves frequent seizures beginning in the first three months of life, with abundant epileptic activity that contributes to significant cognitive and motor delay (6,8). It is frequently associated with gross structural brain abnormalities and occasionally with metabolic disorders, which are often genetic in origin (9). Ohtahara Syndrome (OS) is a severe form of early-onset epilepsy characterized by a distinctive electroencephalogram (EEG) pattern known as 'burst-suppression', which consists of periodic high voltage bursts of slow waves mixed with spikes, followed by marked attenuation (10). The frequency of OS is about 1 in 100 000 live births (11). Children with OS typically have multiple seizure types including tonic spasms and focal seizures, which are often refractory to anti-epileptic drugs (12). Affected children may progress onto other epilepsy syndromes such as West Syndrome (6), or they may die in infancy.

Several genes have been implicated in severe early-onset epilepsy. The first reported for OS was the X-linked *ARX* gene, which encodes a developmental transcription factor (13). *De novo* mutations in *STXBP1* (14,15), encoding a protein involved in synaptic vesicle release, in *CDKL5* (16), encoding a serine/threonine kinase, and in ion channel genes *KCNQ2* (17), *SCN2A* (18,19) and *SCN8A* (20) have also been implicated, as have recessive mutations in the glutamate transporter *SLC25A22* (21). However, many OS patients test negative for mutations in these genes, indicating that other genes have yet to be identified. Multiple additional genes have been associated with the broader range of early-onset epilepsies, including genes encoding cytoskeletal components [*SPTAN1* (22)] and proteins involved in signaling [*PLCB1* (23)], DNA repair [*PNKP* (24)] and neurotransmitter synthesis [*PNPO* (25)]. However, clinical testing is limited by the availability and costs of conventional single-gene tests, and thus tends to be restricted to genes that have been associated with the specific type of epilepsy. There is therefore scope to apply a more comprehensive approach to diagnosis using whole-genome methods.

In this study, we sequenced six patients with sporadic severe early-onset epilepsy, and their healthy parents. The patients were selected because traditional clinical molecular genetic approaches had failed to uncover the causal mutation. Four of the children had been diagnosed with OS, and two had severe non-syndromic early-onset epilepsy (NSEOE). Because these six cases were all sporadic, and the families were reported as non-consanguineous, we anticipated that the causal mutation was most likely to be *de novo*, but we also considered the simple, compound and X-linked recessive models.

RESULTS

We sequenced the six trios (Table 1; Supplementary Materials, Note S1) to high coverage on the Illumina HiSeq platform. In searching for the causal mutations, we considered coding variants as well as variants in regulatory regions within 50 kb of known early-onset epilepsy genes (see Materials and Methods). The most plausible causal variant in each trio was a coding mutation, and we report these here. See the Supplementary Materials, Note S2 for a description of candidate variants that were not deemed to be causal.

Patients 1 and 3: *KCNQ2* and *SCN2A*

Two OS cases had *de novo* non-synonymous mutations in genes encoding ion channel subunits, *KCNQ2* and *SCN2A* (Table 1; Supplementary Materials, Fig. S1A and B). The *KCNQ2* mutation, NM_004518:c.C827T:p.T276I, falls in the highly conserved fifth transmembrane segment of the channel that forms part of the pore. It is two amino acids away from the T274M mutation recently described in an OS patient (26). The *SCN2A* mutation in Patient 3, NM_001040143:c.A5558G:p.H1853R, is in the cytosolic C-terminal region of the protein. It falls within the 250 residue domain that binds FGF14, which is required for localization at the axon initial segment (27). Other *de novo* mutations in the cytosolic domains were recently reported in patients with OS (18). These reports provide strong supporting evidence that these *de novo* mutations, which have not been previously reported in any epilepsy patients, are responsible for OS in these children.

Downloaded from http://hmg.oxfordjournals.org/ at Osaka Daigaku Ningen on March 17, 2015

Table 1. Phenotypes and presumed causal mutations in the six trios sequenced

Trio	Phenotype	Age of seizure onset	Current age	Family history	Previous genetic tests	Brain MRI	EEG	Presumed causal mutation	Evidence for pathogenicity
1	OS; severe DD	1 day	5 years	No	arrayCGH, *FRAXA, STXBP1, MECP2, CDKL5, POLG, ARX*	Age 14 days: reduced posterior white matter volume; thin corpus callosum	Age 14 days: Burst suppression	*de novo* in *KCNQ2*: NM_004518:c.C827T: p.T276I	*KCNQ2* previously implicated in OS
2	OS; metopic synostosis; severe DD	1 day	4 years	Paternal great-grandmother and her sister had epilepsy	arrayCGH, *FRAXA, MECP2, CDKL5, STXBP1*	Age 1 year: cerebral atrophy with delayed myelination and hypomyelination	Age 14 days: Burst suppression	Recessive variant in *KCNT1*, homozygous due to UPD9: NM_020822: c.G2896A:p.A966T	*KCNT1* previously implicated in MMPSI and ADNFLE; electrophysiology demonstrated effect on channel current
3	OS; severe DD	14 days	5 years	No	arrayCGH, *CDKL5, ARX, STXBP1*	Age 8 months: cerebral atrophy, delayed & reduced myelination	Age 6 weeks: Burst suppression	*de novo* in *SCN2A*: NM_001040143: c.A5558G:p.H1853R	*SCN2A* previously implicated in OS
4	OS; severe DD	4 weeks	Deceased age 2 years, 4 months	Mother's cousin died of seizures at age 2	arrayCGH, *MECP2, ARX, STXBP1*	Age 9 months: delayed and reduced myelination	Age 3 months: Burst suppression	Simple recessive in *PIGQ*: NM_004204:exon3: c.690-2A>G	Binding partner *PIGA* implicated in similar syndrome; mutation leads to exon skipping and reduced GPI synthesis
5	Severe NSEOE; microcephaly; severe DD	2 days	19 years	No	arrayCGH, *MECP2, UBE3A, TCF4*	Microcephalic (OFC <3rd percentile); structurally normal brain	Age 8 years: multifocal seizure potential on background of significant disruption of cortical function	*de novo* in *CSNK1G1*: NM_022048:c.C688T: p.R230W	*CSNK1G1* involved in synaptic transmission
6	Severe NSEOE; severe DD; PDA and ASD as neonate; cutaneous hypopigmentation	2.5 months	11 years	No	arrayCGH, *MECP2, CDKL5, STXBP1*	Cerebral hypoplasia; microcephaly (OFC < 0.4th percentile)	Age 6 years: background diffusely of low amplitude, with multifocal sharp waves	*de novo* in *CBL*: NM_005188:exon9: c.1228-1G>A	*CBL* implicated in NCFC syndrome; mutation leads to exon skipping

OS, Ohtahara syndrome; NSEOE, non-syndromic early-onset epilepsy; DD, developmental delay; PDA, patent ductus arteriosis; ASD, atrial septal defect; OFC, occipital frontal cortex; MMPSI, malignant migrating partial seizures of infancy; ADNFLE, autosomal dominant nocturnal frontal lobe epilepsy; GPI, glycosylphosphatidyl inositol; NCFC, neuro-cardio-facial-cutaneous; UPD, uniparental disomy. More detailed clinical descriptions, including seizure types, head circumference and treatments, are given in Supplementary Materials, Note S1.

Downloaded from http://hmg.oxfordjournals.org/ at Osaka Daigaku Ningen on March 17, 2015

Patient 2: *KCNT1*

Patient 2 had very severe early-onset epilepsy, an EEG consistent with OS (Supplementary Material, Fig. S2), and profound developmental delay. He had a paternal family history of childhood idiopathic epilepsy affecting his father's maternal aunt, grandmother and nephew. Patient 2 did not have any compelling *de novo* mutations. However, low chromosomal heterozygosity and detection of multiple Mendelian errors (Fig. 1; Supplementary Materials, Fig. S1C) suggested that he had paternal isodisomy for chromosome 9. This was subsequently confirmed by SNP array (Supplementary Materials, Fig. S3; see Supplementary Materials, Note S3). This finding prompted two new alternative hypotheses: that the patient's symptoms were due to aberrant expression of an imprinted gene on chromosome 9, or that there was a recessive pathogenic mutation on this chromosome that had become homozygous as a result of the isodisomy. There was no evidence in the literature for imprinted genes on this chromosome that had plausible links to epilepsy. We therefore scanned the patient's chromosome 9 for rare homozygous

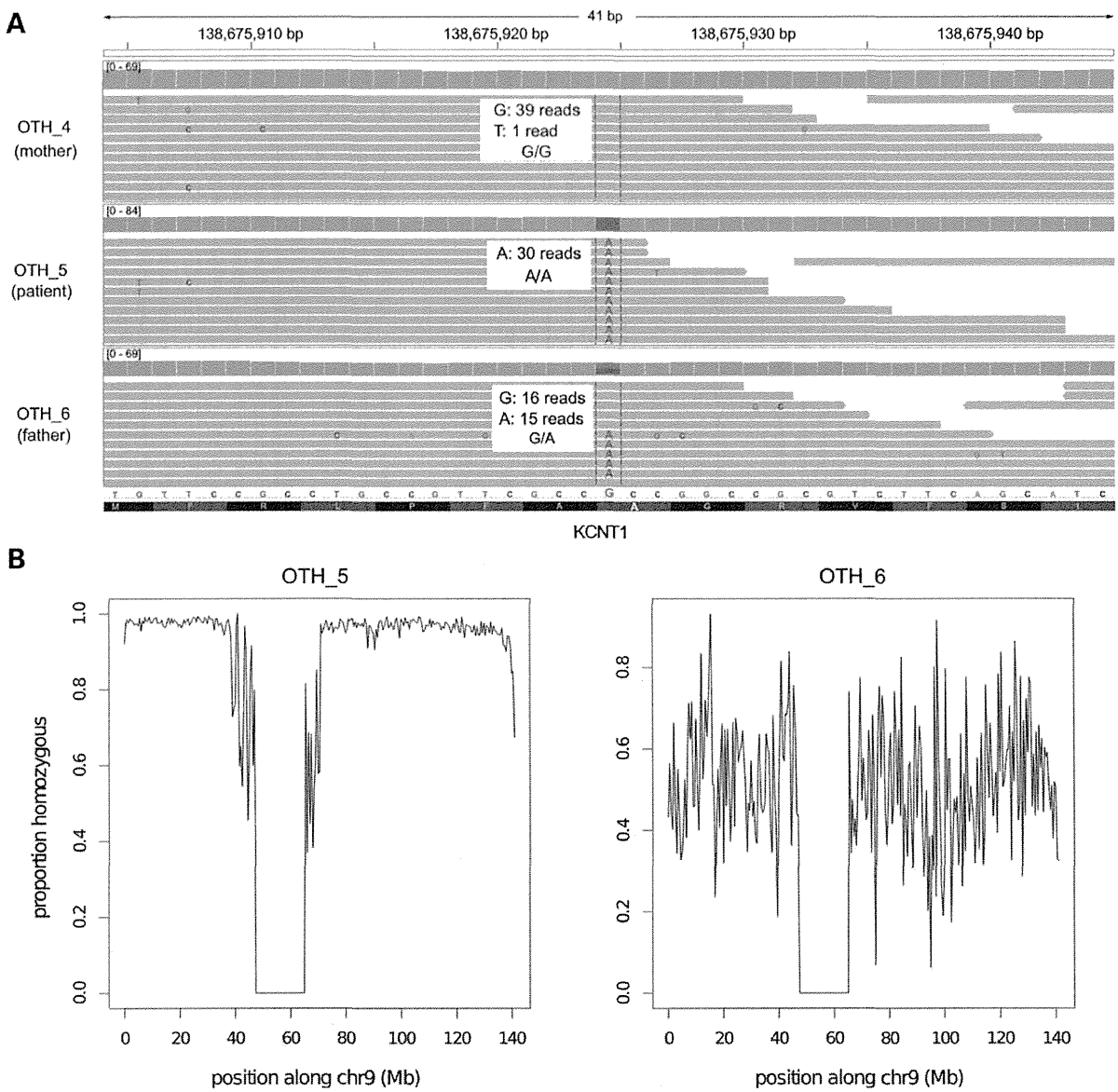

Figure 1. Paternal isodisomy in Patient 2. (**A**) We observed multiple Mendelian errors on chromosome 9 which led us to suspect uniparental disomy (UPD). All variants in the patient (OTH_5) appeared to have been inherited from his father (OTH_6). The *KCNT1* variant is illustrated here as an example. Grey bars represent individual sequencing reads from the sample indicated on the left, and colored letters divergences from the reference sequence. The grey 'pile-up' along the top indicates the sequence coverage. The genotype of each individual is shown. (**B**) These plots show the proportion of variants that are homozygous in 500 kb windows across chr9. OTH_5 was completely homozygous, apart from a few spurious calls; the pattern is similar to that seen on chromosome X in males. His father, OTH_6, is shown for comparison. Note that the dip in the middle represents the centromere.

Downloaded from http://hmg.oxfordjournals.org/ at Osaka Daigaku Ningen on March 17, 2015

variants that might be pathogenic, including around *STXBP1* and *SPTAN1*. The only plausible candidate was a novel non-synonymous variant in *KCNT1* at 9q34.3 that disrupted a highly conserved alanine residue in the intracellular C-terminal domain, NM_020822:c.G2896A:p.A966T. This gene encodes the Na^+-activated K^+ channel known as 'Slack', which is very widely expressed throughout the brain (28). Dominant mutations in *KCNT1* were recently reported to cause autosomal dominant nocturnal frontal lobe epilepsy (ADNFLE) (29), malignant migrating partial seizures of infancy (MMPSI) (30,31) and infantile spasms (32). Interestingly, one of the MMPSI patients with a *KCNT1* mutation was described as having a 'subtle' burst-suppression EEG (30). Distinct from this patient, however, our Patient 2 did not have migrating seizures, and had a clear burst-suppression EEG pattern. Thus, different mutations in *KCNT1* have heterogeneous phenotypic consequences.

The A966 residue in *KCNT1* is completely conserved across all vertebrates for which genome sequences are available. The sequence of the Slack channel C-terminal region is highly conserved between rat and human (92% identical), and residue A966 in the human Slack channel corresponds to residue A945 in the rat protein. We therefore used a rat mutant construct to explore the effect of the novel mutation on channel function, in the same way we described previously for the MMPSI-linked R428Q and A934T mutations (31). We expressed wild-type (WT) and A945T rat Slack in *Xenopus laevis* oocytes, and measured channel activity by performing two-electrode voltage clamping experiments. These experiments showed that activity of the A945T mutant channel was increased significantly by a factor of 13 relative to the WT at +60 mV (Fig. 2A and B). The amounts and integrity of the WT and A945T cRNA used in these experiments appeared similar, just 8% higher in the mutant than the WT (Fig. 2C).

Slack channel activity increases with depolarization (28,33). We therefore compared the voltage dependence of A945T and WT channels. Channel activity of the A945T mutant was significantly greater than that of the WT at all positive potentials (Fig. 2D). However, the voltage dependence of activation of the A945T mutant with depolarization to positive potentials did not differ from that of the WT channel (Fig. 2D) or from that of the previously published reports of Slack channel voltage dependence (31,33). Together, these results suggest that channel opening probability may be greater in the A945T than the WT channel over the same range of depolarized membrane potentials, which would account for the epileptic activity seen in this patient.

Patient 4: *PIGQ*

Patient 4, who was of West African origin, had severe early-onset epilepsy with a burst-suppression EEG, consistent with OS. Although he was reported to be non-consanguineous,

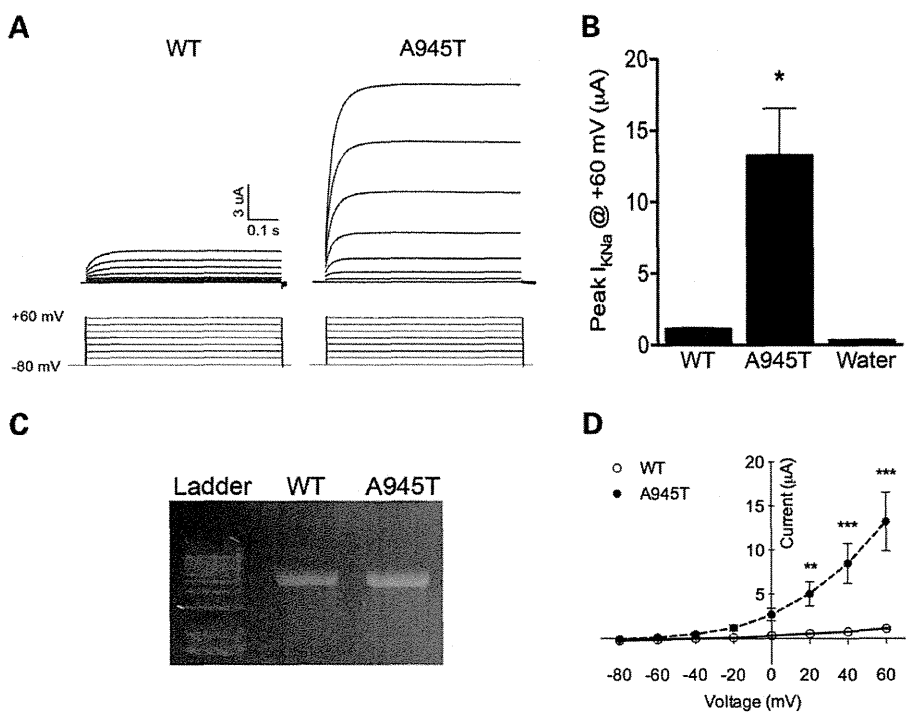

Figure 2. Electrophysiological and channel expression analysis of *KCNT1* mutation found in Patient 2. WT or A945T mutant Slack channel was expressed in *Xenopus laevis* oocytes, and two-electrode voltage clamping (TEVC) performed. (**A**) A representative trace of current activity recorded from an oocyte expressing WT or A945T is shown on top, with the voltage-clamping protocol displayed underneath. (**B**) Averaged quantitation of the peak current is compared at +60 mV ($P < 0.001$, $n = 5$, Student's *t*-test; representative of three independent experiments). (**C**) The quality of RNA injected into *Xenopus* oocytes was checked on a 1% formaldehyde agarose gel. (**D**) Current–voltage relations for the WT or A945T channels. Channel activity as measured at peak current amplitude and normalized to the value at +60 mV is plotted against voltage ($^{**}P < 0.01$, $^{***}P < 0.001$, $n = 5$, two-way ANOVA, Sidak's multiple comparisons test).

Downloaded from http://hmg.oxfordjournals.org/ at Osaka Daigaku Ningen on March 17, 2015

we found several extended homozygous regions in his genome. Within a 2 Mb homozygous region on chr16, he had a novel homozygous single nucleotide variant (SNV) that was predicted to disrupt the highly conserved splice acceptor site of exon 3 of the *PIGQ* gene: NM_004204:exon3:c.690−2A>G. Both parents were heterozygous and two unaffected siblings were either heterozygous or homozygous for the reference allele (Supplementary Materials, Fig. S1D). *PIGQ*, formerly called *GPI1*, encodes a subunit of an *N*-acetylglucosaminyltransferase that catalyzes the first step in glycosylphosphatidyl inositol (GPI) biosynthesis. *PIGQ* stabilizes the enzyme complex (34). A nonsense mutation in the X-linked *PIGA* gene, which encodes another subunit of this enzyme, was recently reported to cause a lethal disorder characterized by multiple congenital abnormalities, structural brain malformations, joint contractures and neonatal seizures with a burst-suppression EEG (35). Recessive mutations in other GPI synthesis genes cause clinically heterogeneous syndromes, all of which involve seizures (36–39). Thus, this *PIGQ* mutation seemed a very plausible candidate for causing OS in Patient 4.

The patient died before we discovered this mutation so we were unable to obtain samples to test the effect of this homozygous mutation on *PIGQ* activity. However, we obtained RNA samples from his parents' blood and examined *PIGQ* splicing. There were two *PIGQ* transcripts, one consistent with the reference annotation and another with a deletion of exon 3, as expected given that the parents were heterozygous for the variant at the splice acceptor site for this exon (Fig. 3A; Supplementary Materials, Fig. S4). Since exon 3 falls immediately before the catalytic domain of *PIGQ*, the mutation seemed likely to abrogate the function of the enzyme and lead to a reduction in GPI synthesis, as was seen for the nonsense mutation in *PIGA* (35). We tested the parents for abnormalities in serum alkaline phosphatase levels and in expression of CD59 on red blood cells, which are typical signs of impaired GPI synthesis (35,36,40), but found none. This is not entirely surprising since heterozygous carriers of other *PIG* gene mutations had normal CD59 levels (37).

The skipping of exon 3 causes an in-frame deletion of 44 amino acids (Fig. 3A). To assess whether this abnormality affected PIGQ function *in vitro*, we transfected human *PIGQ* cDNA either with or without exon 3 into *PIGQ*-deficient Chinese hamster ovary (CHO) cell lines. The mutant *PIGQ* did not restore the surface expression of GPI-anchored proteins (GPI-AP) as efficiently as the WT (Fig. 3B). Additionally, the expression of mutant protein was greatly decreased to a level undetectable by western blotting (Fig. 3C). These results demonstrated that the PIGQ protein lacking the 44 amino acids had some functional activity but was unstable, and so GPI synthesis was impaired. Over 150 proteins have been reported to have GPI anchors (41), including several with important roles in neural development and function (42–44). Further work is needed to determine which of these provides the causal link with epilepsy.

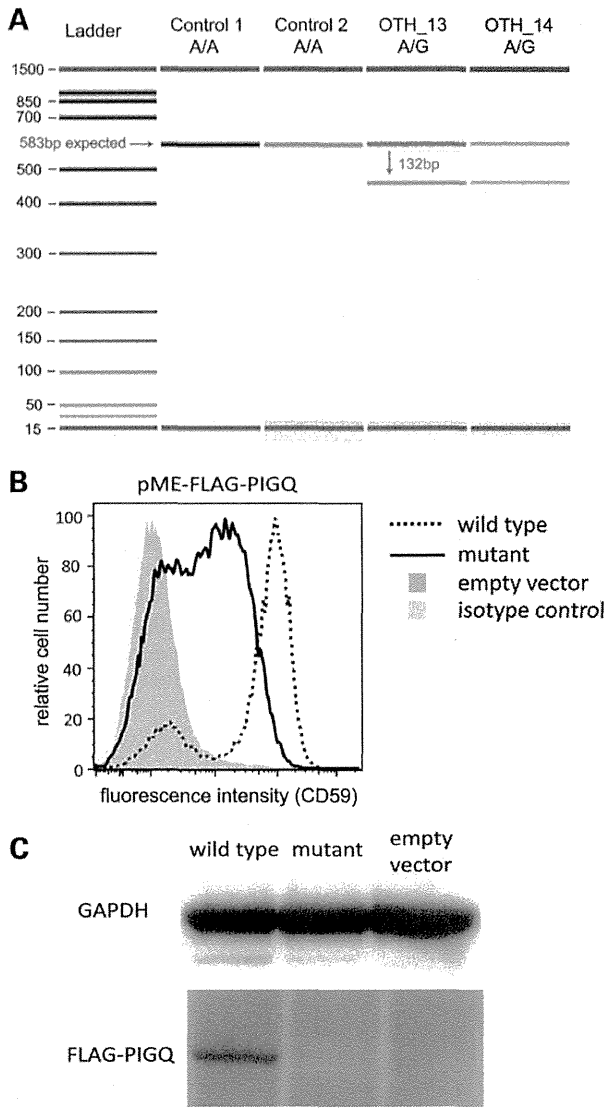

Figure 3. PIGQ splicing mutation in Patient 4. (**A**) The variant causes skipping of exon 3. This image shows the Bioanalyzer gel from an RT-PCR (see Materials and Methods) and demonstrates the presence of two PIGQ transcripts in the heterozygous parents (OTH_13, OTH_14). The blue arrow indicates the band expected from the annotated transcript, and the red arrow that expected from the skipping of exon 3. (**B**) Severely decreased functional activity of the mutant *PIGQ*. *PIGQ*-deficient CHO cells were transiently transfected with WT or mutant *PIGQ* cDNA (lacking exon 3). Restoration of the surface expression of CD59, a GPI-anchored protein, was assessed by flow cytometry after staining with anti-CD59 antibody. The mutant *PIGQ* did not restore the surface expression of CD59 as efficiently as the WT. X axis, fluorescence intensity corresponding to CD59 expression level per cell; Y axis, relative cell number. (**C**) The expression of mutant protein was greatly decreased and could not be detected by western blotting.

Patient 5: *CSNK1G1*

Patient 5 had severe tonic-clonic epilepsy, microcephaly and developmental delay. We found a *de novo* non-synonymous mutation at a highly conserved site in *CSNK1G1* (NM_022048: c.C688T:p.R230W; Supplementary Materials, Fig. S1E). This gene encodes casein kinase 1 (CK1), gamma 1, a serine/threonine kinase expressed in many tissues including the brain. CK1 regulates the phosphorylation of NMDA receptors and is thus important for synaptic transmission (45) (see Supplementary Materials, Note S4). The *CSNK1G1* mutation is a prime

Downloaded from http://hmg.oxfordjournals.org/ at Osaka Daigaku Ningen on March 17, 2015

candidate in this patient, but genetic validation studies did not find any additional patients (see below) and further work is needed to definitively establish it as causal.

Patient 6: *CBL*

Patient 6 had severe tonic epilepsy, microcephaly and developmental delay. We detected a *de novo* mutation in a highly conserved splice site in the *CBL* gene (NM_005188:exon9: c.1228-1G>A), and showed that this led to exon skipping (Supplementary Materials, Fig. S5). Cbl is a ubiquitously expressed adaptor molecule and ubiquitin ligase that regulates the Ras/MAPK pathway (46). It is primarily recognized as a tumor suppressor (47), but germline mutations in it and other genes involved in the Ras/MAPK pathway can also cause various developmental disorders collectively known as the neuro-cardio-facial-cutaneous (NCFC) syndromes or 'RASopathies' (48). Notably, mutations in *KRAS* and *BRAF* were recently reported in two boys with refractory epilepsy and cardio-facial-cutaneous (CFC) syndrome (49). It is likely that this splicing mutation ablates Cbl's ubiquitin ligase activity, thereby over-stimulating Ras/MAPK signaling. This may have disrupted neuronal development and led to severe epilepsy (more details in Supplementary Materials, Note S4).

The patient was reviewed by a number of clinical geneticists. Hypopigmented skin lesions and a history of congenital heart disease were noted, but the clinical diagnosis of a NCFC was not considered likely. Review after this molecular finding did not affect the clinical diagnosis and this patient is still thought not to fit phenotypically into this group of disorders. If this gene is confirmed to be causal, this will widen further the phenotype of the Ras-MAPK disorders.

Mutation screening in other cases

Using a targeted resequencing approach (50), we screened *KCNT1*, *PIGQ*, *CBL* and *CSNK1G1* in a large cohort of epileptic encephalopathy cases from Australia (Supplementary Materials, Table S1). This included two cases of OS, five of early myoclonic encephalopathy [EME; a syndrome which shares features with OS but which is predominantly myoclonic in nature (51)], and thirty-eight of early-onset epileptic encephalopathy (defined as onset within the first three months of life). We also screened these genes in thirteen other cases of OS and EME (Supplementary Materials, Table S2) from a UK cohort, using Sanger sequencing. We looked for coding variants that would fit a recessive model in *KCNT1* and *PIGQ*, or a *de novo* model in *CBL* and *CSNK1G1*, as was observed in our patients, but found none. Two of the OS cases have subsequently been attributed to mutations in other genes (50). Thus, our failure to replicate our findings likely reflects further genetic heterogeneity in severe early-onset epilepsy. We also appreciate the relatively small number of patients we have screened who had similar phenotypes to those described here (total sixteen OS, six EME).

DISCUSSION

WGS heralds promise as a tool for clinical diagnosis of patients with genetic disease. As part of a wide-ranging program to evaluate the clinical utility of WGS (WGS500), we sequenced six patients with severe early-onset epilepsy who had evaded molecular diagnosis by conventional single-gene clinical screening. In doing so, we identified two new genes for OS, as well as two putative genes for severe early-onset epilepsy. This increases the number of known genes for OS from six [*STXBP1* (14), *ARX* (13), *CDKL5* (16), *KCNQ2* (26), *SCN2A* (18) and *SLC25A22* (52)] to eight (adding *KCNT1* and *PIGQ*). In two cases, we found an unexpected inheritance mechanism: uniparental disomy of chromosome 9 in Patient 2, and simple recessive inheritance due to likely distant consanguinity in Patient 4.

Of particular interest was the discovery that Patient 2 had a pathogenic mutation in *KCNT1* that became homozygous through isodisomy. To date, there have been two published cases of homozygous mutations due to isodisomy causing syndromes involving seizures (53,54), but no examples of such mutations causing severe epilepsy. This is also the first reported case of paternal isodisomy for chromosome 9, and of an apparently recessive mutation in *KCNT1*; recently reported mutations causing MMPSI (31), ADNFLE (29) and infantile spasms (55) were all dominant. Nevertheless, we note that, while this mutation appears to be acting in a recessive manner, there was a paternal history of mild idiopathic epilepsy. It is possible that, in the heterozygous state, this variant predisposes to milder epilepsy, but further testing of affected family members was not possible.

The Slack *KCNT1* A945T mutation had a gain-of-function effect on channel activity. Although the two previously characterized MMPSI-causing mutations, R409Q and A913T, were also gain-of-function alterations, the A945T mutation appears to have a much more profound effect. Whereas channel activity was increased by a factor of 3 at +60 mV in the two MMPSI mutant channels (31), the corresponding increase was 13-fold for the A945T mutation. This observation raises the possibility that the patterns of neuronal firing that produce the distinctive EEG patterns characteristic of these different disorders can vary as a function of *KCNT1* channel activity, and can furthermore influence the nature, severity and onset of the seizures.

The *PIGQ* finding emphasizes the importance of the GPI pathway in brain development and function. This gene was not initially considered as a candidate, since the patient did not have the congenital abnormalities found in children with other *PIG* gene mutations, such as polydactyly. However, it became a very plausible candidate after its binding partner, *PIGA*, was reported to cause a lethal disorder involving neonatal seizures (35). We then demonstrated that the *PIGQ* mutation impairs GPI synthesis in a similar manner (Fig. 3). It remains an open question as to how defective GPI synthesis causes epilepsy, although a number of mechanisms have been suggested, including impaired *Cripto* signaling leading to aberrant forebrain development (44), and disruption of contactin-mediated organization of axonal subdomains at the node of Ranvier (42).

We have also made some unexpected findings about the etiology of other non-syndromic forms of early-onset epilepsy. Although the mutations in patients 5 and 6 have not been definitively established as causal, our results point to several interesting pathways not generally associated with epilepsy. The *de novo* splicing mutation in *CBL* in Patient 6 implies that this patient's condition is actually a 'RAS-opathy' (56), which may be consistent with her congenital heart disease. Other genes in the Ras/MAPK pathway have been reported to cause

Downloaded from http://hmg.oxfordjournals.org/ at Osaka Daigaku Ningen on March 17, 2015